International Conference on Renewable Energies and Power Quality (ICREPQ'18)
Salamanca (Spain), 21th to 23th March, 2018
Renewable Energy and Power Quality Journal (RE&PQJ)
ISSN 2172-038 X, No.16 April 2018

System for detection of clouds moving toward the Sun in the sky

P. Sukič, G. Štumberger

Faculty of Electrical Engineering and Computer Science, University of Maribor, Koroška 46, SI-2000, Maribor, Slovenia
e-mail: p.sukic@um.si, gorazd.stumberger@um.si

Abstract. The paper proposes a system for detection of clouds moving toward the Sun. Its aim is to recognize the clouds that will cover the Sun in the next minute and to reduce the output power of the photovoltaic (PV) power plant smoothly and with prescribed dynamics. Since the target cost of the proposed system is in the rage of the cost of a single PV module, it consists of low costs components: a Raspberry PI Model B 3 with a WiFi connection, an OmniVision OV5647 sensor with a wide-angle lens, a circular polarizing (CPL) filter and a natural density (ND) filter. The algorithm for the prediction of cloud movement has been developed for the implementation on the target components and requires low computational effort. Experimental results obtained with the prototype of the proposed system are presented in the paper.

Key words

photovoltaic power plant; cloud passing forecasting; Raspberry Pi; camera;

1. Introduction

The active power produced in a photovoltaic (PV) power plant depends on the solar irradiance. The clouds moving in the sky with high speed can cover the Sun, which can lead to high dynamics in the PV power plant output power. According to the authors in [1–3], these high dynamic changes can cause voltage fluctuations in the electricity networks with a substantial share of installed PV power plants, which could also lead to stability problems. The impact of PV power plants on the distribution network voltages can be effectively reduced passively, using conductors with a larger cross section, or actively, by the introduction of storage systems [3–7]. An alternative to the aforementioned and costly solutions is the predictive reduction of PV power plant output power, based on a reliable prediction of moving clouds that will cover the Sun. When predicting the movement of the clouds, photos of the sky are taken in predefined and constant time steps. In each photo, the Sun and the clouds have to be identified. Based on the changing positions of the clouds their velocity vectors are determined and the time, when they will cover the Sun, is estimated. In [9,10], the authors applied image processing of sky images in order to estimate the solar radiation. The could cover measurements are performed in [11]. The intra-hour cloud tracking is reported in [12], whilst [13] deals with the image based cloud detection and classification.

This paper deals with a system that predicts when the clouds moving toward the Sun will actually cover the Sun. It focusses on those clouds that will cover the Sun in less than one minute which substantially limits the area of observation on the close vicinity of the Sun. If the system detects that a cloud will cover the Sun in the predefined time, shorter than one minute, it starts the procedure that smoothly and with predefined dynamics reduces the PV power plant output power.

The procedure that predicts when a cloud will cover the Sun is based on the signal processing performed on a sequence of sky photos taken in time-equidistant points. In each photo, the Sun is identified first, followed by the identification of clouds in close vicinity of the Sun. The area of observation is reduced to the surroundings of the cloud part closest to the Sun. Based on the change of the cloud, inside this area, in the successively taken photos, the cloud movement vector is determined. It is used to predict the direction and speed of the moving cloud. This data is afterwards used to predict the time when the cloud will cover the Sun. A detailed description of the applied image processing is given in [14].

The main guideline in the development of the discussed system is its wide applicability, which means that its price should be low, not exceeding the price of a single PV module. Thus, the prototype is built around widely available and low-cost components.

The testing of the prototype was performed on a PV power plant operating under real operating conditions over a period of several months. The prototype output signal was compared to the measured output power of a PV power plant. The results presented in this paper show a very good agreement between the output signal of the prototype, which predicts the decrease of the PV power plant output power, due to the clouds that will cover the Sun, and the measured output power.

The outline of the paper is as follows. The second section describes the hardware components of the system. The signal processing procedure, consisting of several sub-procedures, is described in the third section. The experimental results obtained during the testing of the prototype are presented in the section four, whilst the conclusions are drawn in the fifth section.

2. System design constrains and hardware selection

The system was designed considering several constraints. The system must be able to take photos of the sky without sunshade elements and recognize the clouds in close vicinity of the Sun in all conditions. It must be realized without moving parts whilst its price should not exceed the price of a single normal size PV module.
Based on the given constraints following hardware components have been chosen: Raspberry Pi Model B 3 (1.2 GHz 64-bit quad-core ARMv8 CPU and 802.12n Wireless LAN) and the wide-angle lens Waveshare RPI Camera (G), based on the OV5647 sensor, which is additionally equipped with circular polarizing (CPL) and natural density (ND) optical filters mounted in front of the lens. The ND filter prevents saturation of the sensor whilst the CPL filter reduces the flare [13]. The estimated cost for all described components does not exceed 70 €. These hardware components were integrated in the prototype of the proposed system that is shown in Figure 1. In the prototype, the hardware components are used to acquire the time-equidistant sequences of sky photos, which are afterwards used in the image processing, applied to predict the time when the cloud will cover the Sun.

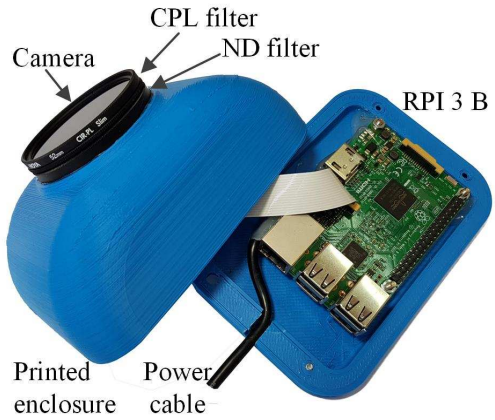

Fig. 1. Hardware components integrated in the prototype

3. Detection of clouds moving toward the Sun in the sky

In order to predict the time in which a moving cloud will cover the Sun several steps are required. After the photo is taken, the Sun is recognized in the photo. In order to minimize the required computation power for image processing, the photo is cropped down to a narrow area around the Sun, in which the moving clouds can cover the Sun in a time shorter than one minute. In the cropped photo the clouds are identified. The checkpoints placed around the Sun are used to detect the presence of the cloud closest to the Sun. An area of interest is defined around the checkpoint where the presence of a cloud is detected. The parts of the area of interests in the two successively taken photos is used to determine the cloud moving vector. It is used to predict the time in which the clouds moving toward the Sun will cover the Sun. A more detailed description of image processing is given in [14].

A. Determining the position of the Sun

A photo of the sky is a suitable input for the image processing if the sensor was not saturated and the flare was reduced to an acceptably low level. This can be achieved by a proper selection of the CPL and ND optical filters, which was a quite demanding task that required a lot of experimental work to find the correct settings.
Each pixel in the photo is described with RGB (Red Green Blue) color values between 0 and 255. For the Sun, these values exceed 250 for the all three colors. However, since the flare problem, that is more pronounced in the red color, cannot be completely eliminated by CPL and ND filters, only values of the green and blue colors are considered to identify the pixels in the photo belonging to the Sun. All pixels for which the sum of the RGB values for the green and blue colors exceeds the value of 500 are considered being part of the Sun. The center of gravity, of all pixels belonging to the area identified as the Sun, is determined by separately summing up the x and y coordinates of these pixels and dividing the obtained sums by the number of pixels. The coordinates of the

center of gravity (x_{sun}, y_{sun}) are considered being the Sun's center.

In some cases, the Sun can be covered by translucent clouds as shown in Figure 2. Thus, an area larger than the actual Sun's size can be identified as the Sun, which could lead to a shift of the identified Sun's center. The predefined minimal and maximal number of the pixels, that can belong to the area identified as the Sun in the photo, is used to limit the error in the identified coordinates of the Sun's center.

Fig. 2. The sun covered by a partially translucent cloud

The area around the Sun's center in the photo is cropped down in order to reduce the size of the photo that will be involved in the further image processing. The size of the copped down area of the photo is determined in such a way, that the clouds, crossing the area's border and moving at maximal speed, cannot cower the Sun in a time shorter than one minute. In the rest of the paper, the cropped down area of the entire photo is referred to as the photo. In this way, the size of the photo involved in the image processing is substantially reduced. This approach also reduces the required computation power which is crucial for the implementation on widely spread low cost hardware components.

B. Identification of Clouds

The identification of the clouds in the sky photos is normally based on the *RBR* (Red Blue Ratio) [8,10] where the photo is decomposed in the Red, Green and Blue (RGB) colors. Since, the reflection is most pronounced in the red color, the identification of the areas in the photo, that are covered by clouds, is in this work based on the Green Blue Ratio (*GBR*). In this way, the problems, caused by the reflection, in the cloud identification procedure are effectively solved.

Each pixel in the photo is decomposed in the Red (R), Green (G) and Blue (B) colors, with values between 0 and 255. If the Green/Blue ratio exceeds the experimentally determined value of 1.2 ($GBR>1.2$) the pixel is identified as a part of a cloud. Each pixel of the photo is represented by an element of the cloud matrix **C** containing logical values 0 and 1. If the pixel is identified as a part of a cloud ($GBR>1.2$), the corresponding element in the cloud matrix **C** is set to the logical value 1. The identification of clouds in the vicinity of the Sun could be disturbed by the scattering of light, caused by the atmosphere. Therefore, all elements in the cloud matrix **C**, with a distance from the Sun's center lower than 2 to 4 times the Sun's radius, are set to the logical value 0. Birds, airplanes and other objects in the sky can disturb the cloud identification. Therefore, only sufficiently large groups of pixels, where also the neighboring pixels are identified as a cloud, are included in the cloud matrix **C**.

C. Detection of clouds in the vicinity of the Sun

In order to detect the presence of clouds in the vicinity of the Sun in a photo, checkpoints are arranged around the Sun's center as shown in Figure 3. The checkpoints are organized in the form of

a checkpoint matrix, the indices of which are marked in Figure 3. The checkpoint matrix contains 4 rows with 32 columns. Each row corresponds to one of 4 in radial direction equidistantly placed orbits (layers), where each orbit (layer) contains 32 angularly equidistantly placed checkpoints.

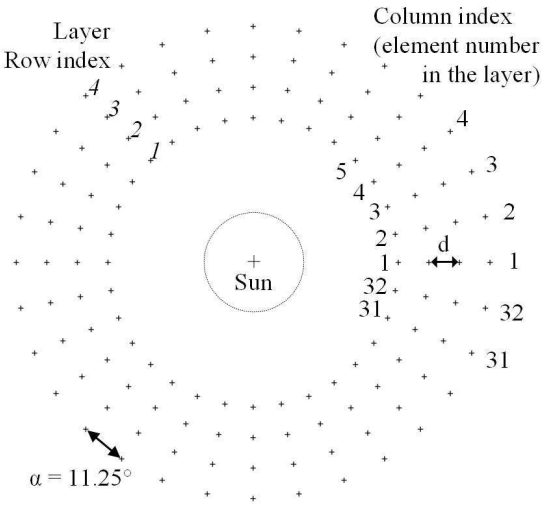

Figure 3. Checkpoints and the checkpoint matrix indices

The procedure for determining the presence of clouds in the vicinity of the Sun starts with the element 1 in the orbit (layer) 1. If the pixel in the cloud matrix **C,** corresponding to the coordinates of the checkpoint, contains the logical value 1, the logical value of the corresponding checkpoint matrix element is also set to 1, which means that the given checkpoint is covered by a cloud. The described procedure is repeated for all elements in the given layer before it starts to check the next layer of checkpoints. If the presence of a cloud is not confirmed in any of the checkpoints, the procedure stops. It starts again when a new photo of the sky is taken.

D. Determining the cloud movement vector

If the presence of a cloud is detected at the given checkpoint, the checkpoint coordinates (x_{posit}, y_{posit}) are stored and the procedure for determining the cloud movement vector starts. The area of interest, with the center at (x_{posit}, y_{posit}) and with a surface of (2 m × 2 m) pixels, is bounded by the closed polygon (x_{posit} -m, y_{posit} -m), (x_{posit} +m, y_{posit} -m), (x_{posit} +m, y_{posit} +m), (x_{posit} -m, y_{posit} +m), (x_{posit} -m, y_{posit} -m), shown in Figure 4. The number of pixels m is selected in such a way, that the area of interest includes at least three checkpoints at the external checkpoint layer.

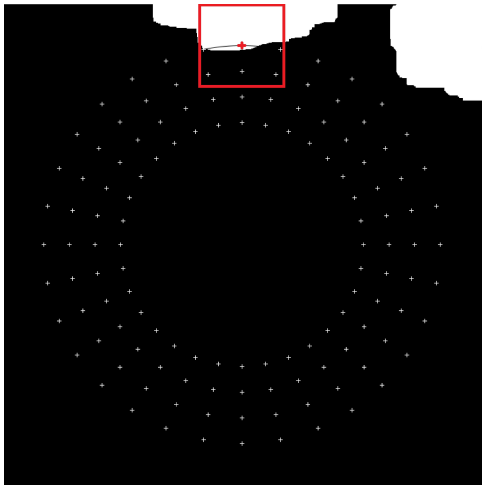

Figure 4. The checkpoint covered by a cloud and the area of interest

Inside the defined area of interests the center of gravity is determined only for those pixles that are marked as a cloud in the cloud matrix **C**. The coordinates of the center of gravity for the photo (i-1) are (x_{ave_p}(i-1), y_{ave_p}(i-1)). With the time delay t_p the next photo with the index i is taken. For this photo, the cloud matrix **C** is determined and in the already defined area of interest the center of gravity coordinates (x_{ave_p}(i), y_{ave_p}(i)) are determined. The difference in the center of gravity coordinates (x_{ave_p}(i), y_{ave_p}(i)) and (x_{ave_p}(i-1), y_{ave_p}(i-1)) is used to determine the cloud movement vector (x_v,y_v), defined by the equations (1) and (2), which describes the cloud's movement.

$$x_v = x_{ave_p}(i-1) - x_{ave_p}(i) \quad (1)$$

$$y_v = y_{ave_p}(i-1) - y_{ave_p}(i) \quad (2)$$

The angle γ, that describes the direction of the cloud's movement, is defined by (3) to (6).

$$\gamma = \arctan\left(\frac{y_v}{x_v}\right);\ x_v > 0 \quad (3)$$

$$\gamma = (\arctan\left(\frac{y_v}{x_v}\right) + \pi);(x_v < 0)\ \&\ (y_v \geq 0) \quad (4)$$

$$\gamma = (\arctan\left(\frac{y_v}{x_v}\right) + \pi)\frac{180}{\pi};(x_v < 0)\ \&\ (y_v < 0) \quad (5)$$

$$\gamma = 90;(x_v = 0)\ \&\ (y_v > 0) \quad (6)$$

Figure 5.a shows the photo of the sky with the index (*i*-1). Figure 5.b shows the next photo of the sky with the index *i*. A straight line with the angle γ, starting at the center of gravity (x_{ave_p}(*i*-1), y_{ave_p}(*i*-1)) is shown in green color in Figure 5.b. A line, parallel to the green line, that starts at the Sun's center (x_{sun}, y_{sun}) is shown in yellow color in Figure 5.b.

E. Identifying the clouds that will cover the Sun

If a cloud is detected in the vicinity of the Sun, it can shortly cover the Sun or it can pass by. In order to distinct between these two cases the angle γ, defined by (3) to (6), is applied. A straight line starting at the Sun's center (x_{sun}, y_{sun}) is defined by (7), where (x_p, y_p) are the pixel coordinates along the straight line in the direction defined by the angle γ, whilst *r* is the radius that increases in the steps of one pixel. Its initial value equals the radius of the first orbit of checkpoints (Layer 1 in Figure 3) whilst its maximal value is marked with r_{max}.

$$\begin{aligned} x_p &= x_{sun} + r\cdot\cos(\gamma) \\ y_p &= y_{sun} + r\cdot\sin(\gamma) \end{aligned} \quad (r = r_1,\ r_1+1,\ r_1+2,\ \ldots,\ r_{max}) \quad (7)$$

For each value of the increasing radius *r*, the corresponding coordinates of the pixel (x_p, y_p) are used to check their status in the cloud matrix **C**. The first pixel that belongs to a cloud, defines the distance between the Sun's center and the cloud *r*(*i*-1) for the actual sky photo with the index (*i*-1). In the same way, the distance between the Sun's center and the cloud *r*(*i*) is determined for the next sky photo with the index *i*. The distances between the Sun's center and the cloud *r*(*i*-1) and *r*(*i*), corresponding to the two successively taken sky photos with the indices (*i*-1*)* and *i*, are shown in Figures 5.b and 5.c in yellow color.

F. Estimated time in which the Sun will be covered by a cloud

Let (*i*-1) and *i* be the indices of the two successively taken sky photos and t_p the time difference in which both photos are taken. Considering the corresponding distances between the Sun's center and a cloud *r*(*i*-1) and *r*(*i*) the predicted time t_{prd} in which the cloud will cover the Sun can be calculated by (8).

$$t_{prd} = \frac{t_p \cdot r(i-1)}{r(i-1) - r(i)} \quad (8)$$

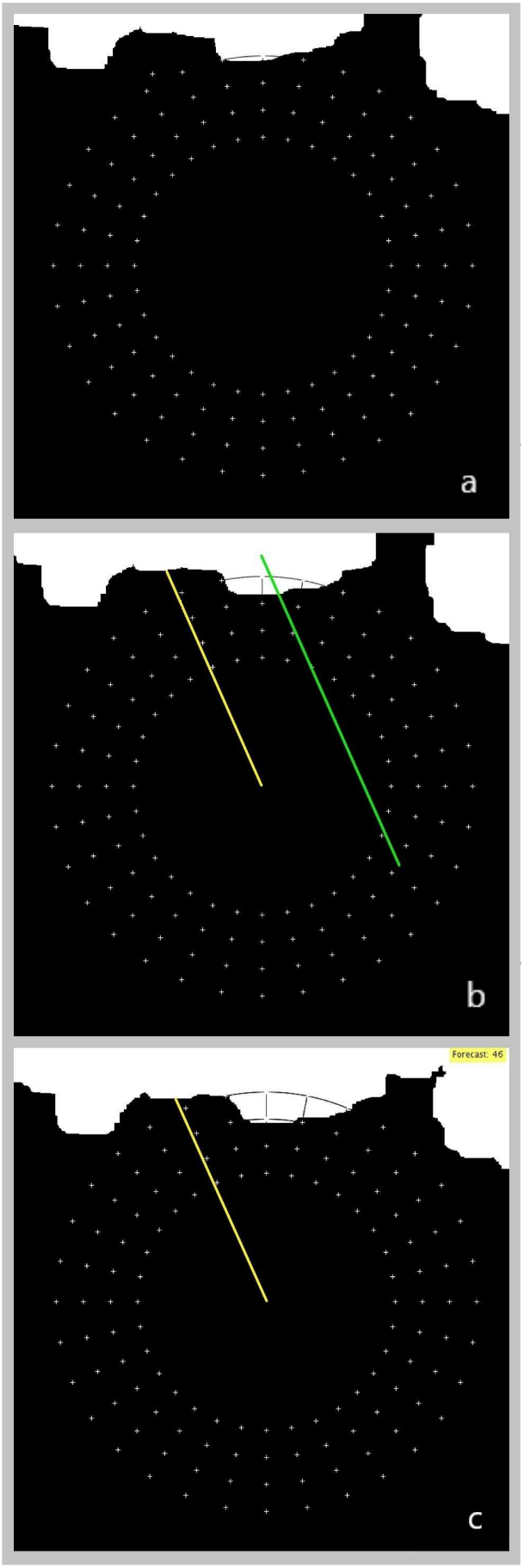

Figure 5. Photos of the sky with the Sun, cloud, checkpoints and marked direction in which the cloud moves

If the estimated time t_{prd} (8), in which the cloud will cover the Sun is in the range of 30 to 60 s, a procedure for a smooth and controlled reduction of the PV power plant output power can be started, where the dynamics of all changes can be prescribed. However, if the estimated time t_{prd} exceeds 60 s, the clouds move at a low speed, and there is enough time to repeat the entire procedure and estimate the time again with better accuracy. If the clouds move slowly, it makes no sense to reduce the output power in advance, since those clouds cannot cause fast changes in the output power.

4. **Results**

Figures 6 and 7 show the output signal generated by the proposed system for the detection of clouds moving toward the Sun, together with the measured output power of a 3.75 kWp experimental PV system installed at the University of Maribor. The PV system is equipped with micro inverters able to accept the reference values for reactive power generation and active power curtailment, which exceeds the scope of this paper. The output power of the PV system is presented in the per unit system. When the developed prototype detects that a cloud will cover the Sun in 30 s or less, the logical value on its output changes from the logical value 0 to the logical value 1. This signal can be used to start the procedure for the reduction of the PV power plant output power. The results presented in Figure 6 clearly show that the predicted time in which the cloud will cover the Sun is correct. 30 s after the signal for the programmed reduction of the PV power plant output power is generated, a cloud covers the Sun and

the output power decreases. Figure 7 shows the same variables as shown in Figure 6. The only difference is that the results in Figure 7 show the results of the prototype testing over the course of a day.

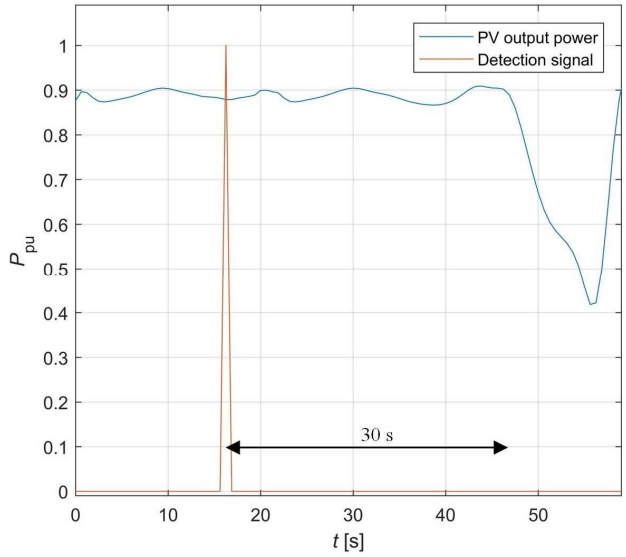

Figure 6. Output signal generated by the prototype of the proposed system and the measured output power of the test PV system

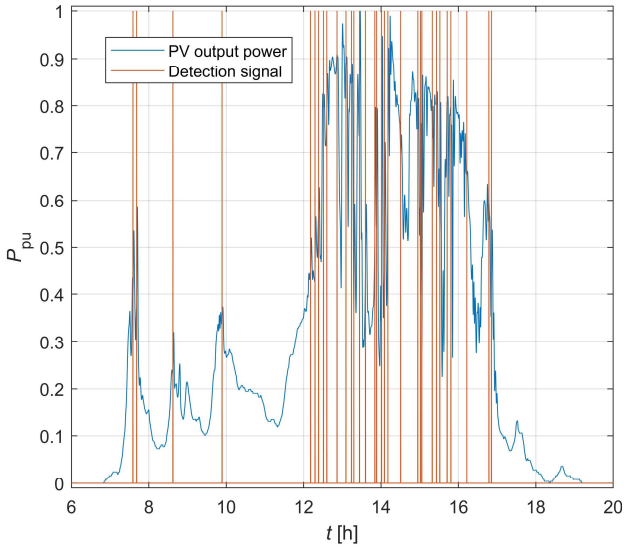

Figure 7. Output signal generated by the prototype of the proposed system and the measured output power of the test PV system

5. Conclusions

This paper deals with a low-cost system that can be applied to avoid fast changes in the output power of PV power plants which could cause voltage fluctuations in electricity networks with a high share of PV power plants. Based on the output signal of the proposed system, all changes in the output power can be smooth with prescribed dynamics.

The developed system estimates the time in which a cloud will cover the Sun which would cause a fast change in the output power of a PV power plant. It is based on widely available, widely used and cheap hardware components. The developed image processing algorithms require low computational effort and are suitable for implementation on the low-cost target hardware components.

The developed prototype reliably estimates the time in which a cloud will cover the Sun for the time span of one minute, whilst its costs are under the costs for a single 250 to 300 Wp PV module

Acknowledgement

This work was partly supported by the Slovenian Research Agency under grants L2-5489 and P2-0115.

References

[1] E. H. Thomas and P. Richard, „Quantifying PV power Output Variability", *Solar Energy* , pp. 1782-1793, 10/2010.

[2] S. Sayeef, S. Heslop, D. Cornforth, T. Moore, P. S., J. Ward and A. Berry, „Solar Intermittency: Australia's Clean Energy Challenge:Characterising the Effect of High Penetration Solar Intermittency onAustralian Electricity Networks", CSIRO, 2012.

[3] S. Shivashankar, S. Mekhilef, H. Mokhlis and M. Karimi, „Mitigating methods of power fluctuation of photovoltaic (PV) sources – A review", *Renewable and Sustainable Energy Reviews*, vol. 59, pp. 1170-1184, 2016.

[4] F. Cheng, S. Willard, j. Hawkins, B. Arellano and A. Mammoli, „Applying battery energy storage to enhance the benefits of photovoltaics", v *Energytech, 2012*, Cleveland, 2012.

[5] A. Ellis, D. Schoenwald, J. Hawkins, S. Willard and B. Arellano, „PV output smoothing with energy storage", v *Photovoltaic Specialists Conference*, Austin, 2012.

[6] A. Puri, „Bounds on the smoothing of renewable sources", v *Power & Energy Society General Meeting*, Denver, 2015.

[7] A. Puri, „Optimally smoothing output of PV farms", v *PES General Meeting*, Harbor, 2014.

[8] C. W. Chow, B. Urquhart, M. Lave, A. Dominguez and B. Washom, „Intra-hour forecasting with a total sky imager at the UC San Diego solar energy testbed", *Solar Energy*, vol. 11, pp. 2881-2893, 2011.

[9] J. Alonso-Montesinos and F. Batlles, "The use of a sky camera for solar radiation estimation based on digital image processing", *Energy*, vol. 90, pp. 377-386, 2015.

[10] A. Hammer, D. Heinemann, E. Lorenz and B. Lückehe, „Short-term forecasting of solar radiation: a statistical approach using satellite data", *Solar Energy*, vol. 67, pp. 139-150, 1999.

[11] R. W. Johnson, W. Hering and J. Shields, „Automated Visibility and Cloud Cover Measurements with a Solid State Imaging System", University of California, San Diego, 1989.

[12] R. Marquez and C. Coimbra, „Intra-hour DNI forecasting based on cloud tracking image analysis", *Solar Energy*, Izv. Volume 91, pp. 327-336, 2012.

[13] M. S. Ghonima, B. Urquhart, C. W. Chow, J. E. Shields, A. Cazorla and J. Kleissl, „A method for cloud detection and opacity classification based on ground based sky imagery", *Atmospheric Measurement Techniques*, vol. 5, 2012.

[14] P. Sukič and G. Štumberger, „Intra-minute cloud passing forecasting based on a low cost IOT sensor - a solution for smoothing the output power of PV power plants", *Sensors*, vol. 17, iss. 5, pp. 1-20, 2017.